ChemComm

RSC Publishing

COMMUNICATION

View Article Online
View Journal | View Issue

Cite this: *Chem. Commun.*, 2013, **49**, 11074

Received 13th August 2013,
Accepted 11th October 2013

DOI: 10.1039/c3cc46203j

www.rsc.org/chemcomm

Phosphinate stabilised ZnO and Cu colloidal nanocatalysts for CO_2 hydrogenation to methanol†

N. J. Brown,[a] J. Weiner,[a] K. Hellgardt,[b] M. S. P. Shaffer*[a] and C. K. Williams*[a]

Colloidal solutions of ZnO–Cu nanoparticles can be used as catalysts for the reduction of carbon dioxide with hydrogen. The use of phosphinate ligands for the synthesis of the nanoparticles from organometallic precursors improves the reductive stability and catalytic activity of the system.

The use of carbon dioxide as a raw material is desirable to add value to waste carbon dioxide streams and to exploit a renewable C_1 building block.[1] The development of liquid fuels based on CO_2 reduction, coupled with suitable renewable or off-peak energy sources, is an attractive means to lower dependence on oil reserves and mitigate climate change without requiring the additional land usage and environmental impacts of biofuels.[1d] One such liquid fuel is methanol, produced by the reaction between carbon dioxide and hydrogen.[1d,2] Methanol is already used as a clean burning liquid transport fuel and can be blended with gasoline providing an attractive 'drop-in' substitute with existing fuel infrastructures, as has been successfully implemented in China.[1d,3]

Methanol can be efficiently produced from CO_2–H_2 gas mixtures using heterogeneous Cu/ZnO/Al_2O_3 and various process/pilot studies exemplify this concept.[1d,e,4] Although, these ternary catalysts are more commonly applied for methanol synthesis from *syn*-gas (CO, H_2, CO_2), both isotopic labelling and modelling studies have suggested that the methanol derives from the CO_2 in the *syn*-gas, leading some authors to propose a direct carbon dioxide hydrogenation mechanism.[5] Recent studies of these *syn*-gas heterogeneous catalysts have shown that the relative loadings of ZnO : Cu and the interface between them are key features to control in order to maximise activity.[6] Such catalysts are synthesized *via* high temperature co-precipitation methods, the formation of zincian malachite, and subsequent reductions.[6a,b] Such methods limit both the degree of ZnO/Cu size control, because of the high temperatures required, and the relative loadings, due to the intrinsic thermodynamic stabilities of the minerals. Recently, Tsang *et al.*, described an alternative catalyst preparation, whereby isolated nanoparticles of ZnO and Cu are ground together to yield highly active heterogeneous catalysts for carbon dioxide hydrogenation.[7] These promising results highlight the potential for nanoparticle syntheses able to control, on the nanometre scale, the size and composition of the Cu and ZnO components. So far, the catalysts tested for CO_2 hydrogenation to methanol have been heterogeneous species, however, in the area of CO hydrogenation (*syn*-gas) to methanol, recent reports have highlighted the potential utility of colloidal solutions/suspensions of nanoparticles, generated under elevated temperatures/pressures and stabilised using excess surfactants.[8]

Here, a series of new colloidal ZnO and Cu nanoparticle catalysts, coordinated by stearate and phosphinate ligands, are prepared using low quantities (sub-stoichiometric *vs.* Zn/Cu) of capping ligands, in order to maximise accessibility for reagents and catalyst components to the nanoparticle surfaces. The active catalyst is prepared by simply mixing solutions of ZnO and Cu nanoparticles; the approach avoids pre-reduction steps/catalyst conditioning and enables facile control of the catalyst compositions (ZnO : Cu). One potential disadvantage is that the approach may limit the direct interface between the two phases; on the other hand, it should allow for dynamic particle collision/contact and potentially self-assembly *in situ*.

The soluble ZnO nanoparticles were prepared by hydrolysing a mixture of Et_2Zn, with sub-stoichiometric quantities of an inorganic zinc complex, *e.g.* $Zn(O_2CR)_2$, where R = stearate.[9] $Zn(O_2CR)_2$, is stable to hydrolysis, due to its lower pK_a value, and therefore serves as a covalent ligand for the ZnO nanoparticle surfaces, without the need for excess free surfactant. This synthesis yielded crystalline ZnO nanoparticles,[9] capped with stearate groups, with sizes 3–4 nm. The nanoparticles show good solubility in solvents such as toluene, ethers and alcohols. Copper nanoparticles have been primarily synthesised by the reduction of inorganic copper(II) salts ($CuSO_4$), with hydrazine hydrate, in the presence of an excess of a neutral coordinating surfactant such as an alkyl-amine.[10] However, copper nanoparticles directly coordinated by anionic ligands ought to be more stable than surfactant stabilised species. Therefore, copper nanoparticles, with stearate ligands were formed by the reaction of Cu(stearate)$_2$, in squalane solution at 60 °C, with two equivalents of hydrazine, dissolved in THF. The resulting deep red solutions of

[a] *Department of Chemistry, Imperial College London, London. E-mail: c.k.williams@imperial.ac.uk, m.shaffer@imperial.ac.uk*
[b] *Department of Chemical Engineering, Imperial College London, London*

† Electronic supplementary information (ESI) available. See DOI: 10.1039/c3cc46203j

copper nanoparticles were stable, under a nitrogen atmosphere, for weeks without any noticeable degradation, as evidenced by UV-Vis and visual inspection (>8 weeks). UV-Vis spectroscopy confirmed the formation of <10 nm sized copper nanoparticles, as a surface plasmon band was clearly observed at 580 nm (Fig. S1, ESI†).[10,11] TGA confirmed the presence of the stearate ligand, with ~90% mass loss between 200 and 300 °C (Fig. S2, ESI†) corresponding to the expected particle composition (Cu = 12.5%, see ESI†). The TEM images of the nanoparticles (Fig. S3, ESI†) showed that most of the particles were very small (diameters <10 nm, mean 5.3 nm ± 0.5 nm, although very small sub-nm clusters may not be included) and were well dispersed (see ESI† for more information on Cu particle size determination using DLS, Fig. S17, ESI†).

Mixtures of the stearate-capped ZnO and Cu nanoparticles, dissolved in squalane, were applied as catalysts for the reaction of carbon dioxide and hydrogen reaction. The catalyst solutions were tested at 50 bar (3 : 1 H_2 : CO_2) and 523 K, under continuous gas flows of 166 STP mL min^{-1}. The reaction was highly selective: the major product being methanol and the only by-product was a small amount of carbon monoxide (1–3 μmol h^{-1}). Using either ZnO or Cu nanoparticles on their own led to very low activities, an efficient catalyst was only formed by mixing the two components together (Table 1, catalyst system **1**). The catalysts all showed activation periods of approximately 2 hours (at which point the peak activity is reported). The catalysts were benchmarked against an activated commercial Cu/ZnO/Al_2O_3 catalyst, suspended in squalane (see ESI,† for activation details). The stearate capped nanoparticle catalysts show lower activities than the ternary control, though it's worth noting that the optimum composition of 65 : 35 ZnO : Cu (w/w) has less copper than typically ternary systems.

Although promising activities were exhibited, the post-reaction solution contained significant quantities of a red precipitate, which became green on isolation and exposure to air. These observations suggested that the catalyst structures were changing during the reaction and, indeed, TEM analysis of the isolated, post-reaction red particles, showed ripening of both the ZnO and Cu nanoparticles, with average particle diameters increasing from 1–5 nm, to 10–30 nm (Fig. S5, ESI†). This ripening was also accompanied by a loss of methanol activity. Control experiments using only stearate-capped zinc oxide exposed to hydrogen gas (30 bar H_2, 473 K, 75 mL min^{-1}), showed increased particle agglomeration (Fig. S6, ESI†). Furthermore, mass spectrometry analysis enabled detection of long-chain alcohol products, consistent with reduction of the stearate functionalities. Thus an alternative capping ligand is needed with greater reductive stability. Dialkyl phosphinates potentially satisfy this requirement, whilst maintaining the same overall anionic charge and related coordination modes. Furthermore, the two alkyl groups may improve nanoparticle solubility compared to the single chain of a carboxylate. Additionally, there is precedent for dialkyl phosphinic acids being used as surfactants in the synthesis of CdSe nanoparticles, which also crystallize in wurtzite forms.[12] However, there are not yet any reports of di(alkyl)phosphinate-capped ZnO nanoparticles.

Table 1 Catalytic activities of the stearate-capped ZnO and Cu nanoparticles for methanol production, at different proportions, by weight, of ZnO : Cu

Catalyst system[a]	ZnO : Cu (w/w)[b]	Activity[b]/μmol g^{-1} h^{-1}
Ternary reference[c]	35 : 65	7371
Cu(0)(stearate)	0 : 100	<1
ZnO (stearate)	100 : 0	<1
1	25 : 75	3201
1	35 : 65	5611
1	50 : 50	4931
1	65 : 35	6275
1	75 : 25	2728

[a] Reaction conditions: 523 K, 50 bar (3 : 1, H_2 : CO_2), in squalane, at a fixed total volume of 104 mL, a total gas flow of 166 mL min^{-1}, over 16 h. [b] See ESI for calculations. [c] Alfa Aesar ternary methanol synthesis catalyst (product code: 45 776), comprising (by weight) 25% ZnO, 65% CuO, 10% Al_2O_3 and MgO (*i.e.* 35 : 65, ZnO : Cu). The catalyst is activated as per the method described in the ESI.

The low temperature organometallic synthesis route was modified to prepare a series of ZnO nanoparticles, capped with di(octyl)phosphinate moieties. The nanoparticles produced by this route were similar to the stearate capped ZnO nanoparticles (by ATR-IR, UV-Vis spectroscopy, microscopy, TGA and XRD, see ESI† for details) and were also soluble in organic solvents, such as toluene (16 g L^{-1}, 298 K). They were sufficiently soluble as to enable analysis by NMR spectroscopy. The $^{31}P\{^1H\}$NMR spectrum, in CD_2Cl_2, shows a single resonance at 57 ppm (Fig. S11, ESI†), shifted *vs.* free dioctyl phosphinic acid (60 ppm) and zinc bis(di(octyl)phosphinate) (52 ppm); VT-NMR studies (LT) did not change the resonance. The NMR data indicate that the phosphinate groups are coordinated to the zinc oxide surface. The TGA data indicate that a full monolayer of phosphinate binds to the surface (see ESI† for details).[9c] The relatively large size and cone angle of this ligand, together with IR spectroscopic data (Fig. S7, ESI†), suggest that a significant proportion of the surface zinc atoms are –OH terminated, and are therefore available as catalytic sites. As hoped, the phosphinate ligated ZnO nanoparticles were much more stable (TEM, Fig. S13, ESI†) than the stearate-capped analogues (Fig. S6, ESI†) when exposed to hydrogen gas (30 bar H_2, 488 K, 2 h).

The catalytic activities of these di(octyl)phosphinate-capped zinc oxide nanoparticles, mixed with stearate-capped copper nanoparticles, were higher than the stearate-capped analogues, regardless of the composition of the mixture. Once again, the optimum composition corresponded to a 65 : 35, ZnO : Cu ratio (Table 2). At this loading, the activity of phosphinate-capped ZnO exceed by ~3 times those for either the stearate-capped ZnO nanoparticles or the ternary catalysts (Fig. S16, ESI†).

Next, the best catalyst system was examined before and after reaction (Table 2, entry 3). In contrast to the experiments using the stearate-capped ZnO nanoparticles, the post-reaction mixture using the di(octyl)phosphinate-capped ZnO catalysts remained a clear red solution (Fig. 1). The UV-Vis spectrum (toluene) showed characteristic absorptions for both ZnO (<400 nm) and Cu (580 nm) nanoparticles (Fig. S14, ESI†). This solution was poured into acetone (a non-solvent for both ZnO and Cu nanoparticles) to obtain an air-sensitive, red powder precipitate which was isolated by centrifugation. XRD analysis of this powder showed that both wurtzite ZnO and metallic Cu are present (Fig. S15, ESI†). There is also a broad peak at ~10–20° which is assigned to the organic ligands (di(octyl)phosphinate and stearate) and/or residual squalane. The TEM analysis showed the formation of new,

Table 2 Catalytic activities of the di(octyl)phosphinate capped ZnO and stearate-capped Cu nanoparticles for methanol production, at different proportions, by weight, of ZnO/Cu

Catalyst system[a]	ZnO : Cu (w/w)[a]	Activity[a]/μmol g^{-1} h^{-1}
Ternary reference[a]	35 : 65	7371
2	50 : 50	8584
2	65 : 35	20 356
2	75 : 25	6942
3	65 : 35	1742
4	65 : 35	3578

2 = zinc oxide with di(octyl)phosphinate and copper with stearate capping ligands. **3** = zinc oxide and copper both with di(octyl)phosphinate capping ligands. **4** = zinc oxide with stearate and copper with di(octyl)phosphinate capping ligands. [a] See Table 1.

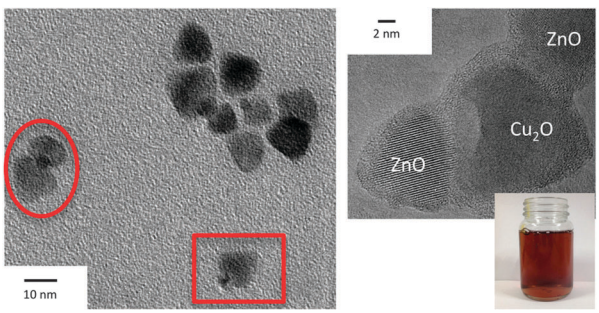

Fig. 1 LHS: TEM image of particles isolated from catalyst 2 (Table 2, entry 3), comprising an initial loading of ZnO : Cu of 65 : 35 (w/w). The highlighted areas illustrate the possible formation of nanostructures between the ZnO and copper particles (Fig. S18, ESI†). RHS (top) shows a HR-TEM image. RHS (bottom) shows a photograph of the red solution obtained after the reaction with no catalyst precipitation observed.

discrete nanostructures. The only limited particle agglomeration (Fig. 1 and Fig. S18, ESI†) may be partly related to sample preparation effects. The HR-TEM image shows zinc oxide nanoparticles, in intimate contact with Cu_2O particles (as identified by lattice spacings); the oxidation of the active copper metal likely occurred through air exposure on the TEM grid. The TEM image shows distinctive nanostructures (marked) which appear to combine one or two pyramidal ZnO particles with a small, equiaxiated copper (oxide) particle (the speciation is inferred from the HR-TEM analysis). Schimpf *et al.*, reported the formation of related, though distinct, 'bow-tie' nanostructures from ZnO/Cu catalysts used for *syn*-gas to methanol catalysts. The apparent presence of related nano-structures in both reactions may point to common catalyst species.[8a]

Other permutations of the ligand systems were less successful. Using di(octyl)phosphinate capping ligands for both zinc oxide and copper nanoparticles reduced the catalytic activity to only ~8% of the best system (Table 2, entry 5). Furthermore, using a catalyst formed by adding stearate-capped zinc oxide to di(octyl)phosphinate-stabilised Cu also reduced activity to just ~17% of the best system (Table 2, entry 6). These findings are consistent with the need to form an interface between the ZnO and Cu nanoparticles to produce high activity catalysts. Thus, when the organic ligands on the copper are too stable (with phosphinate), the copper cannot be deposited on the ZnO surface, conversely, when the ZnO is unstable (with stearate), ripening prevents the formation of a high concentration of the critical ZnO/Cu interface.

The organometallic approach to nanoparticle preparation provides a simple and versatile means of preparing fine structured colloidal catalysts with different compositions, sizes and geometries to conventional systems, whilst avoiding excess free ligand/surfactant in solution. The approach can provide strongly-bound stabilising ligands whilst retaining surface activity. The promising initial activity observed for CO_2 reduction is encouraging, and should motivate further studies of a broad range of related systems and reactions.

Notes and references

1 (*a*) M. Aresta, *Carbon Dioxide as a Chemical Feedstock*, Wiley-VCH, Weinheim, 2010; (*b*) D. J. Darensbourg, *Inorg. Chem.*, 2010, **49**, 10765; (*c*) N. MacDowell, N. Florin, A. Buchard, J. Hallett, A. Galindo, G. Jackson, C. S. Adjiman, C. K. Williams, N. Shah and P. Fennell, *Energy Environ. Sci.*, 2010, **3**, 1645; (*d*) G. A. Olah, *Angew. Chem., Int. Ed.*, 2013, **52**, 104; (*e*) W. Wang, S. P. Wang, X. B. Ma and J. L. Gong, *Chem. Soc. Rev.*, 2011, **40**, 3703.
2 G. A. Olah, A. Goeppert, M. Czaun and G. K. S. Prakash, *J. Am. Chem. Soc.*, 2013, **135**, 648.
3 C.-J. Yang and R. B. Jackson, *Energy Policy*, 2012, **41**, 878.
4 (*a*) G. C. Chinchen, P. J. Denny, J. R. Jennings, M. S. Spencer and K. C. Waugh, *Appl. Catal.*, 1988, **36**, 1; (*b*) L. C. Grabow and M. Mavrikakis, *ACS Catal.*, 2011, **1**, 365; (*c*) F. Pontzen, W. Liebner, V. Gronemann, M. Rothaemel and B. Ahlers, *Catal. Today*, 2011, **171**, 242; (*d*) M. Saito and K. Murata, *Catal. Surv. Asia*, 2004, **8**, 285; (*e*) M. Saito, M. Takeuchi, T. Fujitani, J. Toyir, S. C. Luo, J. G. Wu, H. Mabuse, K. Ushikoshi, K. Mori and T. Watanabe, *Appl. Organomet. Chem.*, 2000, **14**, 763; (*f*) J. G. Wu, M. Saito, M. Takeuchi and T. Watanabe, *Appl. Catal., A*, 2001, **218**, 235.
5 (*a*) G. C. Chinchen, K. C. Waugh and D. A. Whan, *Appl. Catal.*, 1986, **25**, 101; (*b*) G. Dutta, A. A. Sokol, C. R. A. Catlow, T. W. Keal and P. Sherwood, *ChemPhysChem*, 2012, **13**, 3453.
6 (*a*) M. Behrens, *J. Catal.*, 2009, **267**, 24; (*b*) M. Behrens, F. Studt, I. Kasatkin, S. Kuhl, M. Havecker, F. Abild-Pedersen, S. Zander, F. Girgsdies, P. Kurr, B. L. Kniep, M. Tovar, R. W. Fischer, J. K. Norskov and R. Schlogl, *Science*, 2012, **336**, 893; (*c*) P. L. Hansen, J. B. Wagner, S. Helveg, J. R. Rostrup-Nielsen, B. S. Clausen and H. Topsoe, *Science*, 2002, **295**, 2053.
7 (*a*) F. L. Liao, Y. Q. Huang, J. W. Ge, W. R. Zheng, K. Tedsree, P. Collier, X. L. Hong and S. C. Tsang, *Angew. Chem., Int. Ed.*, 2011, **50**, 2162; (*b*) F. L. Liao, Z. Y. Zeng, C. Eley, Q. Lu, X. L. Hong and S. C. E. Tsang, *Angew. Chem., Int. Ed.*, 2012, **51**, 5832; (*c*) X. W. Zhou, J. Qu, F. Xu, J. P. Hu, J. S. Foord, Z. Y. Zeng, X. L. Hong and S. C. E. Tsang, *Chem. Commun.*, 2013, **49**, 1747.
8 (*a*) S. Schimpf, A. Rittermeier, X. Zhang, Z.-A. Li, M. Spasova, M. W. E. van den Berg, M. Farle, Y. Wang, R. A. Fischer and M. Muhler, *ChemCatChem*, 2010, **2**, 214; (*b*) M. K. Schroter, L. Khodeir, M. W. E. van den Berg, T. Hikov, M. Cokoja, S. J. Miao, W. Grunert, M. Muhler and R. A. Fischer, *Chem. Commun.*, 2006, 2498; (*c*) M. A. Sliem, T. Hikov, Z.-A. Li, M. Spasova, M. Farle, D. A. Schmidt, M. Havenith-Newen and R. A. Fischer, *Phys. Chem. Chem. Phys.*, 2010, **12**, 9858; (*d*) M. A. Sliem, S. Turner, D. Heeskens, S. B. Kalidindi, G. Van Tendeloo, M. Muhler and R. A. Fischer, *Phys. Chem. Chem. Phys.*, 2012, **14**, 8170; (*e*) S. Vukojevic, O. Trapp, J. D. Grunwaldt, C. Kiener and F. Schuth, *Angew. Chem., Int. Ed.*, 2005, **44**, 7978; (*f*) J. M. Corker and J. Evans, *J. Chem. Soc., Chem. Commun.*, 1994, 1027.
9 (*a*) A. Gonzalez-Campo, K. L. Orchard, N. Sato, M. S. P. Shaffer and C. K. Williams, *Chem. Commun.*, 2009, 4034; (*b*) K. L. Orchard, J. E. Harris, A. J. P. White, M. S. P. Shaffer and C. K. Williams, *Organometallics*, 2011, **30**, 2223; (*c*) K. L. Orchard, M. S. P. Shaffer and C. K. Williams, *Chem. Mater.*, 2012, **24**, 2443; (*d*) K. L. Orchard, A. J. P. White, M. S. P. Shaffer and C. K. Williams, *Organometallics*, 2009, **28**, 5828.
10 C. Papavassiliou and T. Kokkinakis, *J. Phys. F: Met. Phys.*, 1974, **4**, L67.
11 A. C. Curtis, D. G. Duff, P. P. Edwards, D. A. Jefferson, B. F. G. Johnson, A. I. Kirkland and A. S. Wallace, *J. Phys. Chem.*, 1988, **92**, 2270.
12 (*a*) F. Wang, R. Tang, J. L. F. Kao, S. D. Dingman and W. E. Buhro, *J. Am. Chem. Soc.*, 2009, **131**, 4983; (*b*) C. M. Evans, A. M. Love and E. A. Weiss, *J. Am. Chem. Soc.*, 2012, **134**, 17298.

